

Search for D^0 decays to invisible final states at Belle

Yun-Tsung Lai^{*†}

National Taiwan University

E-mail: ytlai@hep1.phys.ntu.edu.tw

We report the first search for D^0 decays to invisible final states. The measurement result is obtained by using a data sample of 924 fb^{-1} collected at and near the $\Upsilon(4S)$ and $\Upsilon(5S)$ resonances with the Belle detector at the KEKB asymmetric e^+e^- collider. The measured branching fraction will be reported.

VIII International Workshop On Charm Physics
5-9 September, 2016
Bologna, Italy

^{*}Speaker.

[†]On behalf of the Belle Collaboration.

1. Introduction

In the Standard Model (SM), heavy (D or B) meson decay to $\nu\bar{\nu}$ is helicity suppressed [1] with an expectation of branching fraction of $\mathcal{B}(D^0 \rightarrow \nu\bar{\nu}) = 1.1 \times 10^{-30}$ [2], which is beyond the reach of current collider experiments. As estimated in Ref. [1], the branching fraction can be enhanced for the decay of D and B mesons to dark matter (DM) final states, such as two-body decay, radiative decay, and with an additional light meson. With several DM candidates such as ν quark in the hidden valley model [3] and right-handed neutrino [4], the branching fraction of D^0 to invisible final states could be enhanced to as large as $O(10^{-15})$.

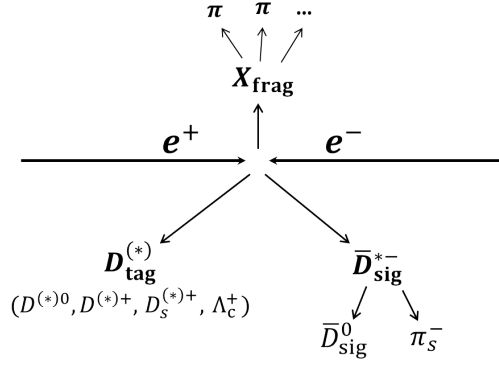
At an e^+e^- flavor factory, two heavy flavor particles are produced in flavor-conjugate states. With fully reconstructing one of the D or B mesons, the recoil information can be utilized to search for the D or B meson decay to an invisible final state. This search for $D^0 \rightarrow$ invisible decay with the charm tagger method at B factories provides an alternative way for searching for DM. Any clear signal would be an indication for new physics. Measurements of B^0 decays to invisible final states with both hadronic and semileptonic B tagging methods are already reported by both Belle and BaBar experiments [5, 6].

We use the data sample of 924 fb^{-1} collected at or near the $\Upsilon(4S)$ and $\Upsilon(5S)$ resonances with the Belle detector [7] at the KEKB asymmetric-energy e^+e^- collider [8]. The Belle detector is a large-solid-angle magnetic spectrometer that consists of a silicon vertex detector (SVD), a 50-layer central drift chamber (CDC), an array of aerogel threshold Cherenkov counters (ACC), a barrel-like arrangement of time-of-flight scintillation counters (TOF) and an electromagnetic calorimeter (ECL) comprised of CsI(Tl) crystals located inside a superconducting solenoid that provides a 1.5 T magnetic field. An iron flux-return yoke located outside the solenoid is instrumented to detect K_L^0 mesons and to identify muons. The detector is described in detail elsewhere [7].

2. Charm tagger method

In order to identify D^0 decays involving invisible particles, we use the charm tagger method to select an inclusive D^0 sample [9, 10, 11, 12] by reconstructing the process $e^+e^- \rightarrow c\bar{c} \rightarrow D_{\text{tag}}^{(*)} X_{\text{frag}} \bar{D}_{\text{sig}}^{*-}$ with $\bar{D}_{\text{sig}}^{*-} \rightarrow \bar{D}_{\text{sig}}^0 \pi_s^-$, except for \bar{D}_{sig}^0 . An illustration of the method is shown in Figure 1. Here, $D_{\text{tag}}^{(*)}$ represents a charmed particle used as a tag: $D^{(*)0}$, $D^{(*)+}$, $D_s^{(*)+}$, or Λ_c^+ . Since the center-of-mass (c.m.) energy of KEKB is above the open charm threshold, a fragmentation system (X_{frag}) with a few light mesons can also be produced. The π_s^- denotes a charged pion from $\bar{D}_{\text{sig}}^{*-}$ decay.

We use the final-state particles: π^+ , K^+ , p , γ , $\pi^0 \rightarrow \gamma\gamma$, $K_S^0 \rightarrow \pi^+\pi^-$, $\Lambda \rightarrow p\pi^-$ for the reconstruction in the charm tagger. The detection for the charged particles are based on information obtained from the tracking systems (SVD and CDC) and the hadron identification systems (CDC, ACC, and TOF). The photon is reconstructed from the energy cluster in the ECL which is not associated with a charged track. The decay modes for D_{tag} , D_{tag}^* , and X_{frag} system are listed in Table 1, 2, and 3, respectively. For each $D_{\text{tag}}^{(*)} X_{\text{frag}}$ candidate, a π_s^- is selected from the remaining tracks. The \bar{D}_{sig}^0 momentum is defined as the missing momentum recoiling against $D_{\text{tag}}^{(*)} X_{\text{frag}} \pi_s^-$ in the c.m. frame. A fit is performed by constraining $M_{\text{miss}}(D_{\text{tag}}^{(*)} X_{\text{frag}})$ to the nominal D^{*+} mass

**Figure 1:** An illustration of the charm tagger method.

($m_{D^{*+}}$) [13] in order to improve the resolution of $M_{D^0} \equiv M_{\text{miss}}(D_{\text{tag}}^{(*)} X_{\text{frag}} \pi_s^-)$. If more than one $\bar{D}_{\text{sig}}^{*-}$ candidate is found in an event, we choose the one with the smallest χ^2 , which is obtained from the fit with $M_{\text{miss}}(D_{\text{tag}}^{(*)} X_{\text{frag}})$ constrained to $m_{D^{*+}}$. If more than one \bar{D}_{sig}^0 candidate is found in an event, we choose the one with largest opening angle between \bar{D}_{sig}^0 and $D_{\text{tag}}^{(*)}$ in the c.m. frame.

Table 1: D_{tag} decay modes.

D^0 decay	D^+ decay	Λ_c^+ decay	D_s^+ decay
$K^- \pi^+$	$K^- \pi^+ \pi^+$	$p K^- \pi^+$	$K^+ K^- \pi^+$
$K^- \pi^+ \pi^0$	$K^- \pi^+ \pi^+ \pi^0$	$p K^- \pi^+ \pi^0$	$K_S^0 K^+$
$K^- \pi^- \pi^+ \pi^+$	$K_S^0 \pi^+$	$p K_S^0$	$K_S^0 K_S^0 \pi^+$
$K^- \pi^- \pi^+ \pi^+ \pi^0$	$K_S^0 \pi^+ \pi^0$	$\Lambda \pi^+$	$K^+ K^- \pi^+ \pi^0$
$K_S^0 \pi^+ \pi^-$	$K_S^0 \pi^+ \pi^+ \pi^-$	$\Lambda \pi^+ \pi^0$	$K_S^0 K^- \pi^+ \pi^+$
$K_S^0 \pi^+ \pi^- \pi^0$	$K^+ K^- \pi^+$	$\Lambda \pi^+ \pi^+ \pi^-$	

Table 2: D_{tag}^* decay modes.

D^{*+} decay	D^0 decay	D_s^{*+} decay
$D^0 \pi^+$	$D^0 \pi^0$	$D_s^+ \gamma$
$D^+ \pi^0$	$D^0 \gamma$	

The inclusive D^0 yield is extracted from a one-dimensional extended unbinned maximum likelihood fit, with the likelihood defined as

$$\mathcal{L} = \frac{e^{-\sum_j N_j}}{N!} \prod_{i=1}^N (\sum_j N_j P_j(M_{D^0}^i)), \quad (2.1)$$

where N is the total number of candidates, N_j is the number of events in component j , $M_{D^0}^i$ is M_{D^0} value of the i -th candidate, and P_j represents the corresponding one-dimensional probability

Table 3: X_{frag} system for $D_{\text{tag}}^{(*)}$.

$D^{(*)+}$	$D^{(*)0}$	Λ_c^+	$D_s^{(*)+}$	
nothing(K^+K^-)	$\pi^+(K^+K^-)$	$\pi^+\bar{p}$	$K_S^0,$	$\pi^0 K_S^0$
$\pi^0(K^+K^-)$	$\pi^+\pi^0(K^+K^-)$	$\pi^+\pi^0\bar{p}$	$\pi^+K^-,$	$\pi^+\pi^0K^-$
$\pi^+\pi^-(K^+K^-)$	$\pi^+\pi^-\pi^+(K^+K^-)$	$\pi^+\pi^-\pi^+\bar{p}$	$\pi^+\pi^-K_S^0,$	$\pi^+\pi^-\pi^0K_S^0$
$\pi^+\pi^-\pi^0(K^+K^-)$			$\pi^+\pi^-\pi^+K^-$	

density function (PDF). The fit includes two components: inclusive D^0 signal and the background. The fit is shown in Figure 2, and we obtain 694505_{-1472}^{+1030} inclusive D^0 decays.

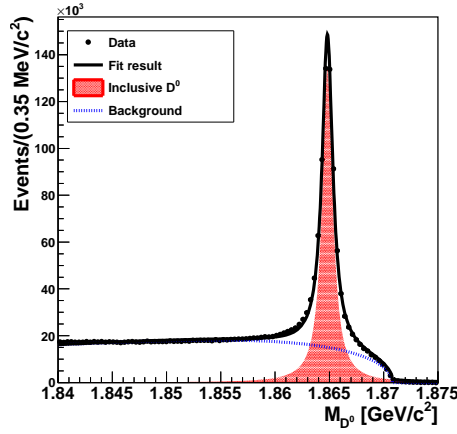


Figure 2: M_{D^0} distribution of the inclusive D^0 sample. The points with error bars are data; the solid line is the fit result; the blue dotted line is background, and the red area is the inclusive D^0 signal.

3. Measurement on $D^0 \rightarrow$ invisible decays

Invisible D^0 decays candidate is identified by requiring no remaining final-state particles associated with \bar{D}_{sig}^0 : events from the inclusive \bar{D}_{sig}^0 sample with remaining charged tracks, π^0 , K_L^0 , K_S^0 , or Λ are vetoed. In addition to M_{D^0} , the residual energy in the ECL (E_{ECL}) is also used to extract the $D^0 \rightarrow$ invisible signal. E_{ECL} is defined as the sum of the energies of the ECL clusters that are not associated with the particles of the $D_{\text{tag}}^{(*)}X_{\text{frag}}\pi_s^-$ system. In order to suppress the beam background, cluster energies are required to be above ECL-region-dependent minimums: 50 MeV for $32.2^\circ < \theta < 128.7^\circ$, 100 MeV for $\theta < 32.2^\circ$, and 150 MeV for $\theta > 128.7^\circ$.

The backgrounds for $D^0 \rightarrow$ invisible include two types: the D^0 background from the $e^+e^- \rightarrow c\bar{c}$ process in which correctly-tagged D^0 peak in M_{D^0} (e.g. $D^0 \rightarrow K^0\pi^0$); and the non- D^0 background from $e^+e^- \rightarrow q\bar{q}$ ($q = u, d, s, c$), $\Upsilon(4S)$, and $\Upsilon(5S)$ decays.

The signal yield is extracted from a two-dimensional extended unbinned maximum likelihood

fit, with the likelihood defined as

$$\mathcal{L} = \frac{e^{-\sum_j N_j}}{N!} \prod_{i=1}^N (\sum_j N_j P_j(M_{D^0}^i, E_{\text{ECL}}^i)), \quad (3.1)$$

where P_j represents the corresponding two-dimensional PDF, and E_{ECL}^i is the E_{ECL} value of the i -th candidate. The P_j functions are products of M_{D^0} PDFs and E_{ECL} PDFs since correlations between M_{D^0} and E_{ECL} are found to be small. The fit includes three components: signal, D^0 background, and non- D^0 background.

The projections of the fit are shown in Figure 3. The fitted signal yield of $D^0 \rightarrow$ invisible is $-10.2_{-20.8}^{+22.1}$, which is consistent with zero.

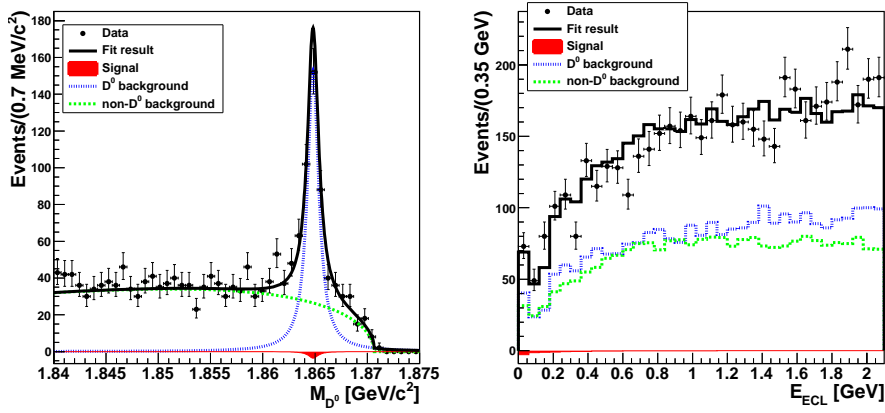


Figure 3: Fit results of D^0 decays to invisible final states. The top plot shows the M_{D^0} distribution for $E_{\text{ECL}} < 0.5 \text{ GeV}$ and the bottom one shows E_{ECL} for $M_{D^0} > 1.86 \text{ GeV}/c^2$. The points with error bars are data; the solid line is the fit result; the blue dotted line is D^0 background; the green dashed line is non- D^0 background, and the red area is signal of D^0 decays to invisible final states.

The branching fraction is calculated using

$$\mathcal{B} = \frac{N_{\text{sig}}}{\epsilon \times N_{D^0}^{\text{incl}}}, \quad (3.2)$$

where N_{sig} , $N_{D^0}^{\text{incl}}$, and ϵ are the fitted signal yield of $D^0 \rightarrow$ invisible decays, the number of inclusive D^0 mesons, and the efficiency of reconstructing $D^0 \rightarrow$ invisible decays within the inclusive D^0 sample, respectively. The reconstruction efficiency is estimated using the MC simulation and a factor $C_{\text{veto}} = 1.1$ is included due to the corrections associated with the vetoes on remaining final state particles in the reconstruction of \bar{D}_{sig}^0 . The C_{veto} value is obtained from a study with $D^0 \rightarrow K^- \pi^+$ control sample described below. The calibrated reconstruction efficiency for the signal is $(62.4_{-3.1}^{+3.2})\%$.

We repeat the entire analysis with the $D^0 \rightarrow K^- \pi^+$ control sample to check the analysis procedures and systematic effects. Exactly the same selection criteria as for the $D^0 \rightarrow$ invisible analysis are applied, except for the two tracks as K^- and π^+ from \bar{D}_{sig}^0 . The projections of the fit for $D^0 \rightarrow K^- \pi^+$ are shown in Figure 4. The efficiency of reconstructing $D^0 \rightarrow K^- \pi^+$ is 29.0%. With

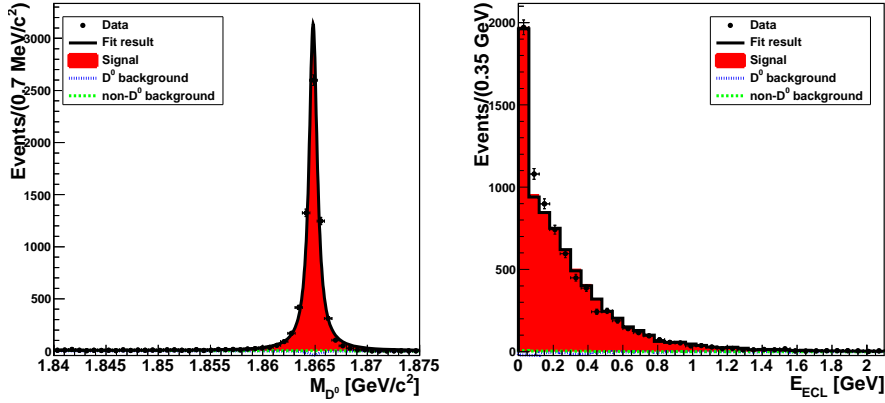


Figure 4: Fit results of $D^0 \rightarrow K^- \pi^+$. The top plot shows the M_{D^0} distribution for $E_{\text{ECL}} < 0.5$ GeV and the bottom one shows E_{ECL} for $M_{D^0} > 1.86$ GeV/ c^2 . The points with error bars are data; the solid line is the fit result; the blue dotted line is D^0 background; the green dashed line is non- D^0 background, and the red area is $D^0 \rightarrow K^- \pi^+$ signal.

a signal yield of 7891^{+125}_{-126} , we obtain $\mathcal{B}(D^0 \rightarrow K^- \pi^+) = (3.92 \pm 0.06(\text{stat.}))\%$, which is consistent with the world average of $(3.93 \pm 0.04)\%$ [13].

Since the observed yield for $D^0 \rightarrow \text{invisible}$ is not significant, we calculate a 90% confidence level Bayesian upper limit on the branching fraction (\mathcal{B}_{UL}) [14]. The upper limit is obtained by integrating the likelihood function:

$$\int_0^{\mathcal{B}_{\text{UL}}} \mathcal{L}(\mathcal{B}) d\mathcal{B} = 0.9 \int_0^1 \mathcal{L}(\mathcal{B}) d\mathcal{B}, \quad (3.3)$$

where $\mathcal{L}(\mathcal{B})$ denotes the likelihood value. The systematic uncertainties summarized in Table 4 are taken into account by replacing $\mathcal{L}(\mathcal{B})$ with a smeared likelihood function:

$$\mathcal{L}_{\text{smeared}}(\mathcal{B}) = \int_0^1 \mathcal{L}(\mathcal{B}') \frac{e^{-\frac{(\mathcal{B}-\mathcal{B}')^2}{2\Delta\mathcal{B}^2}}}{\sqrt{2\pi}\Delta\mathcal{B}} d\mathcal{B}', \quad (3.4)$$

where $\Delta\mathcal{B}$ is the total systematic uncertainty on \mathcal{B}' . We thus determine the upper limit on the branching fraction of $D^0 \rightarrow \text{invisible}$ to be 8.8×10^{-5} at the 90% confidence level.

4. Conclusion

We have performed the first search for D^0 decays into invisible final states with the charm tagger method by using a data sample of 924 fb^{-1} collected by Belle. No significant signal yield is found and we set an upper limit on the branching fraction of 8.8×10^{-5} at the 90% confidence level for the $D^0 \rightarrow \text{invisible}$ decay.

Acknowledgement

We thank the KEKB group and all Belle members for supporting this work and thank the workshop organizer for hosting this meeting.

Table 4: Summary of the systematic uncertainties on the branching fraction.

Source	in %
$N_{D^0}^{\text{incl.}}$	$\pm 0.2(\text{stat.}) \pm 4.9(\text{syst.})$
C_{veto}	+4.7/ -4.6
MC statistics	± 1.9
Total	+7.1/ -7.0

Source	in events
Yield bias	+0.5
Signal PDF in E_{ECL}	+2.3
D^0 background PDF in E_{ECL}	+2.4/ -2.6
Non- D^0 background PDF in E_{ECL}	-12.9
Signal PDF in M_{D^0}	+0.2/ -0.1
Non- D^0 background PDF in M_{D^0}	+0.1
Total	+3.4/ -13.2

References

- [1] A. Badin *et al.*, Phys. Rev. D **82**, 034005 (2010).
- [2] Throughout this paper, inclusion of charge-conjugate decay modes is always implied.
- [3] M. J. Strassler and K. M. Zurek, Phys. Lett. B **651**, 374 (2007).
- [4] H. E. Haber and G. L. Kane, Phys. Rept. **117**, 75 (1985).
- [5] C. L. Hsu *et al.* (Belle Collaboration), Phys. Rev. D **86**, 032002 (2012).
- [6] J. P. Lees *et al.* (BaBar Collaboration), Phys. Rev. D **86**, 051105 (2012).
- [7] A. Abashian *et al.* (Belle Collaboration), Nucl. Instrum. Methods Phys. Res. Sect. A **479**, 117 (2002); also see detector section in J. Brodzicka *et al.*, Prog. Theor. Exp. Phys. (2012) 04D001.
- [8] S. Kurokawa and E. Kikutani, Nucl. Instrum. Methods Phys. Res. Sect. A **499**, 1 (2003), and other papers included in this Volume; T. Abe *et al.*, Prog. Theor. Exp. Phys. **2013**, 03A001 (2013) and references therein.
- [9] L. Widhalm *et al.* (Belle Collaboration), Phys. Rev. Lett. **97**, 061804 (2006).
- [10] L. Widhalm *et al.* (Belle Collaboration), Phys. Rev. Lett. **100**, 241801 (2008).
- [11] A. Zupanc *et al.* (Belle Collaboration), JHEP **09**, 139 (2013).
- [12] P. del Amo Sanchez *et al.* (BaBar Collaboration), Phys. Rev. D **82**, 091103 (2010).
- [13] K.A. Olive *et al.* (Particle Data Group), Chin. Phys. C, **38**, 090001 (2014).
- [14] As we use a Bayesian method, this is formally a ‘‘credibility level’’. However, we use ‘‘confidence level’’ here following common convention.